Applied Surface Science 565 (2021) 150288

Contents lists available at ScienceDirect

Applied Surface Science

journal homepage: www.elsevier.com/locate/apsusc

Full Length Article

Oxidation processes at the surface of $BaTiO_3$ thin films under environmental conditions

Irena Spasojevic [a,b], Guillaume Sauthier [a], José Manuel Caicedo [a], Albert Verdaguer [c], Neus Domingo [a,*]

[a] Catalan Institute of Nanoscience and Nanotechnology (ICN2), CSIC and BIST, Campus UAB, Bellaterra, 08193 Barcelona, Spain
[b] Department of Chemistry, Universitat Autónoma de Barcelona, Bellaterra, 08193 Barcelona, Spain
[c] Institut de Ciència de Materials de Barcelona (ICMAB-CSIC), Campus UAB, Bellaterra, 08193 Barcelona, Spain

ARTICLE INFO

Keywords:
XPS
$BaTiO_3$ thin films
Ferroelectric materials
BaO_2
Surface oxidation
Water splitting

ABSTRACT

Dissociation and adsorption of water on ferroelectric oxide surfaces play important role in the processes of screening and switching dynamics of ferroelectric polarization, as well as in catalytic processes which can be additionally coupled with light, temperature or vibration stimuli. In this work, we present XPS study of ferroelectric $BaTiO_3$ thin films and determine the entanglement between surface chemistry, polarization direction and stability, by observing changes upon time exposure to environmental conditions, heating in O_2 atmosphere and irradiation in vacuum. We devote special attention to Ba 3d spectral region and identify two different oxidation states of O atoms in the compounds of Ba. While this second specie was generally attributed to Ba in surface compounds where it has different oxygen coordination than in the bulk, based on the XPS results of oxygen annealed thin films, we demonstrate that this so far neglected component, corresponds to barium peroxide (BaO_2) and identify it as important active specie for the study of screening mechanisms closely related with catalytic activity present in this ferroelectric material. Finally, we report on chemically assisted polarization switching in thin films induced by heating in vacuum or exposure to X-Ray radiation due to the formation of positive surface electric field created by oxygen or electron vacancies, respectively.

1. Introduction

As one of the commonly found surface adsorbates on all ambient-exposed surfaces, water influences all surface related processes such as catalytic reactions, adhesion [1], friction [2] etc. Particular attention has been devoted to the investigation of adsorbed water and its effects on ferroelectric oxide materials, where due to its dipolar character and ionic conductivity, it has important role in external screening of detrimental depolarization fields [3] and ferroelectric phase stabilization [4]. As a consequence, ferroelectric phase stability [4] and even switching dynamics [5,6] are becoming inevitably coupled to their surface chemical composition. However, the relationship between water and ferroelectric properties is bidirectional: the different polarization states will influence the affinity and sticking coefficients of chemical species on oppositely polarized ferroelectric substrates, as demonstrated from Near-ambient pressure X-Ray photoelectron spectroscopy (NAP-XPS) [7-9] and desorption studies of water and short-chain alcohols [10,11].

Furthermore, water adsorption is strongly influenced by the termination of the oxide layer [12-15], whereby water molecules can adsorb as a whole (molecular adsorption) or dissociate resulting in the formation of hydroxyl ions (OH^-) and protons (H^+) building strong chemical bonds with the metal ions of the substrate [16]. It has been demonstrated that BaO termination of barium titante ($BaTiO_3$) single crystal prompts dissociative adsorption of the first water layer, while in the case of TiO_2 termination dissociative and molecular adsorption might occur [14].

Other less investigated, yet very important, are the electrocatalytical properties of ferroelectric materials, due to the native presence of surface electric fields or when coupled with some external stimuli such as light, change of temperature or vibrations [17-20]. Driven by the need of depolarization fields screening, surface charges can accommodate or supply negative/positive charges and therefore actively take part in surface chemical reactions. On this way, by changing the polarization one can create oxidative or reducing ferroelectric surfaces on demand [21-23].

In order to fully understand complex processes happening at the

* Corresponding author.
E-mail address: neus.domingo@icn2.cat (N. Domingo).

https://doi.org/10.1016/j.apsusc.2021.150288
Received 17 March 2021; Received in revised form 10 May 2021; Accepted 31 May 2021
Available online 3 June 2021

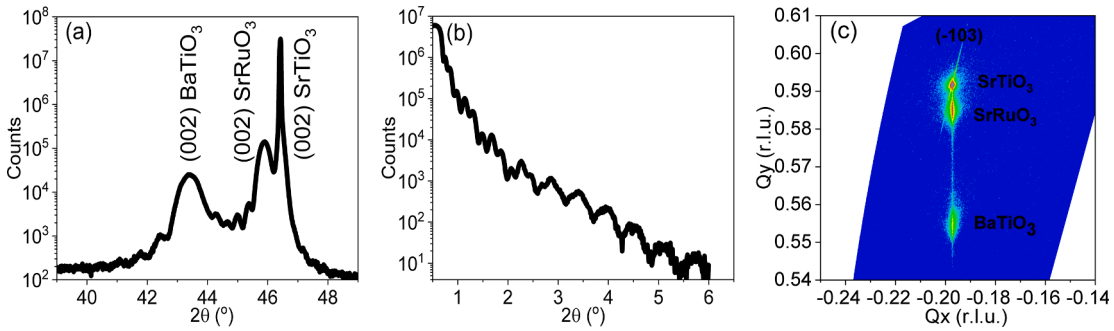

Fig. 1. Results of X-ray diffraction analysis of $SrRuO_3/BaTiO_3$ bilayers grown on $SrTiO_3$ substrate. (a) 2θ/ω coupled scan around the (0 0 2) reflection of the $SrTiO_3$ substrate, $SrRuO_3$ buffer electrode and $BaTiO_3$ thin film, (b) X-Ray reflectivity measurements and (c) X-ray reciprocal space map (XRSM) around (-1 0 3) Bragg peak, showing that $SrRuO_3$ and $BaTiO_3$ layers are coherent and fully strained to $SrTiO_3$ substrate.

ferroelectric surfaces and take advantage of them, it is necessary to identify all the chemical species and their behavior in different experimental conditions and time frames. By means of powerful tools such as NAP-XPS, the presence of species such as molecular water and hydroxyl (OH) groups has been well established [12]. Of particular interest is the detection of surface oxygen species such as metal-peroxo complexes that can appear as intermediate species directly associated with oxidative water splitting reactions [12,24,25]. However, species related with the presence of surface Ba-related compounds have been scarcely studied [26] and in most of the cases they show inconsistent results.

In this report, we present an XPS study of epitaxial and monodomain $BaTiO_3$ thin films exposed to ambient conditions. Beside the expected species, such as molecular water, hydroxyl (OH) groups and different carbon-related species (CO_x) we report on the existence of additional specie, observable as a high energy component in Ba 3d spectral region. Up to know, assignment of this peak is controversial and still under debate: it was generally attributed to Ba in surface compounds in which Ba has different oxygen coordination than in the bulk [27,28], but occasionally it has also been inconsistently assigned to $BaCO_3$ species [29,30]. In order to delve into its origin, we studied the correlation of this peak with all the contributions on the O 1s and C 1s regions, after annealing the thin films in oxygen. Further on, by combined use of XPS and Piezoresponse Force Microscopy (PFM) we studied effect of prolonged atmosphere exposure on oppositely polarized $BaTiO_3$ thin films and observe striking differences in surface chemical composition and hydrophilic character of up- and down- polarized surfaces, which we interpret in the light of enhanced oxidizing activity of down-polarized $BaTiO_3$ thin films. Finally, we report on the observed polarization switching in thin films under different environmental conditions. We observe that after heating in vacuum or exposure to X-Ray radiation the films spontaneously switch the ferroelectric polarization in both cases from up to down-polarized state. We will explain these dynamics in terms of both electrical and chemical modifications of the surface, induced by processes such as the formation of positive surface electric fields created by oxygen or electron vacancies, respectively.

2. Experimental details

2.1. $SrRuO_3$ (SRO)/$BaTiO_3$ (BTO) thin film preparation

Epitaxial ferroelectric $SrRuO_3/BaTiO_3$ bilayers were grown by Pulsed Laser Deposition (PLD) technique on $SrTiO_3$ (STO) substrates. A KrF excimer laser ($\lambda = 248$ nm, fluence 5.4 J/cm^2, 2 Hz repetition rate) was used to ablate stoichiometric ceramic targets of $SrRrO_3$ and $BaTiO_3$. As received (1 0 0) oriented $SrTiO_3$ single crystals (CrysTec GmbH) were used as substrates in all depositions. Target-substrate distance was fixed at 8 cm. Prior to the growth of $BaTiO_3$ layer, we firstly grow $SrRuO_3$ layer which serves as a bottom electrode for PFM measurements. Both $SrRuO_3$ and $BaTiO_3$ layer were deposited in O_2 atmosphere with partial oxygen pressure $pO_2 = 100$ mTorr and at deposition temperatures of 635 °C and 700 °C, respectively. After the deposition sample was cooled down slowly to the room temperature with the rate of 3 °C/min in saturated O_2 atmosphere ($pO_2 = 10^4$ mTorr) in order get rid of any present oxygen vacancies.

2.2. Structural characterization

Structural properties of as grown $BaTiO_3$ thin films were studied by X-Ray diffraction. Coupled 2θ/ω scans around (0 0 2) reflection, X-Ray reflectivity (XRR) and X-Ray reciprocal space map (XRSM) measurements were done on PANalytical X'Pert Pro diffractometer.

2.3. Atomic Force Microscopy (AFM) analysis

AFM imaging was performed on an MFP-3D AFM (Asylum Research). In all the experiments, PPP-EFM tips (Nanosensors) with a stiffness constant k = 2.8 N/m and coated with $PtIr_5$ were used. Topography of the samples was imaged in tapping mode, and ferroelectric properties were probed by Piezoresponse Force Microscopy (PFM) in DART mode and Switching Spectroscopy PFM (SS-PFM).

2.4. XPS measurements

XPS measurements were performed at room temperature with a SPECS PHOIBOS 150 hemispherical analyzer (SPECS GmbH, Berlin, Germany) with a base pressure of $5x10^{-10}$ mbar using monochromatic Al K-alpha radiation (1486.74 eV) as excitation source operated at 300 W. The energy resolution as measured by the FWHM of the Ag $3d_{5/2}$ peak for a sputtered silver foil was 0.62 eV. Some of the samples were annealed in a separate chamber in O_2 atmosphere and then transferred back to the XPS chamber by vacuum suitcase without exposure to the atmosphere. The fitting of the XPS spectra was performed by CasaXPS software after Shirley subtraction of the background with a combination of Gaussian/Lorentzian functions in a ratio 70:30 for all peaks. Deconvolution of the spectra in the O 1s, C 1s, Ba $3d_{5/2}$ and Ti 2p regions is described in detail in the text. In order to compare spectra obtained from different samples, O 1s spectra were normalized by the intensity of the bulk oxide peak, while for Ba $3d_{5/2}$ and C 1s spectra, the BaO $3d_{5/2}$ and Ti 2p peak intensities were used.

3. Results and discussion

3.1. Structural, ferroelectric and surface characterization of $SrRuO_3$/$BaTiO_3$ thin films

Structural properties of as grown $BaTiO_3$ thin films were studied by X-Ray diffraction in 2 theta/omega (2θ/ω) geometry, whereby ω and 2θ denote incident and diffracted angle, respectively. High resolution 2θ/ω

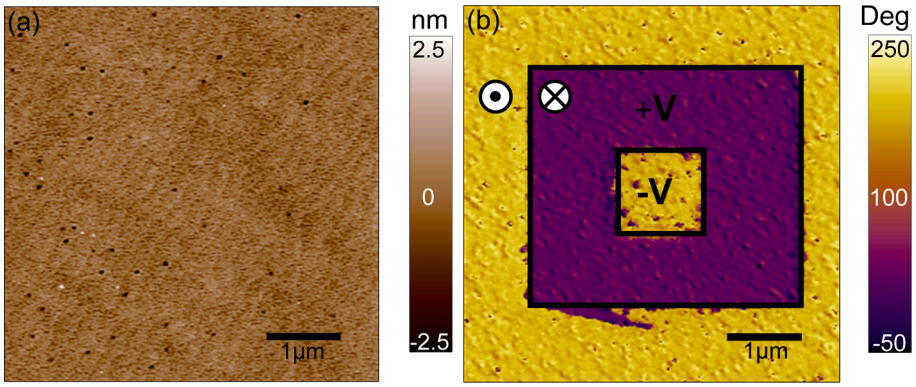

Fig. 2. (a) AFM topography of a 5 x 5 μm^2 area showing the atomic steps of a perfectly layered sample. (b) PFM Phase image of the as-grown up polarized area, where a squared pattern of 3.5 × 3.5 μm^2 has been switched to down polarization (purple area) by applying a positive voltage of V_{tip} = 8 V and switched back to up polarization with a reversed voltage of V_{tip} = − 8 V (yellow squared inset). (For interpretation of the references to colour in this figure legend, the reader is referred to the web version of this article.)

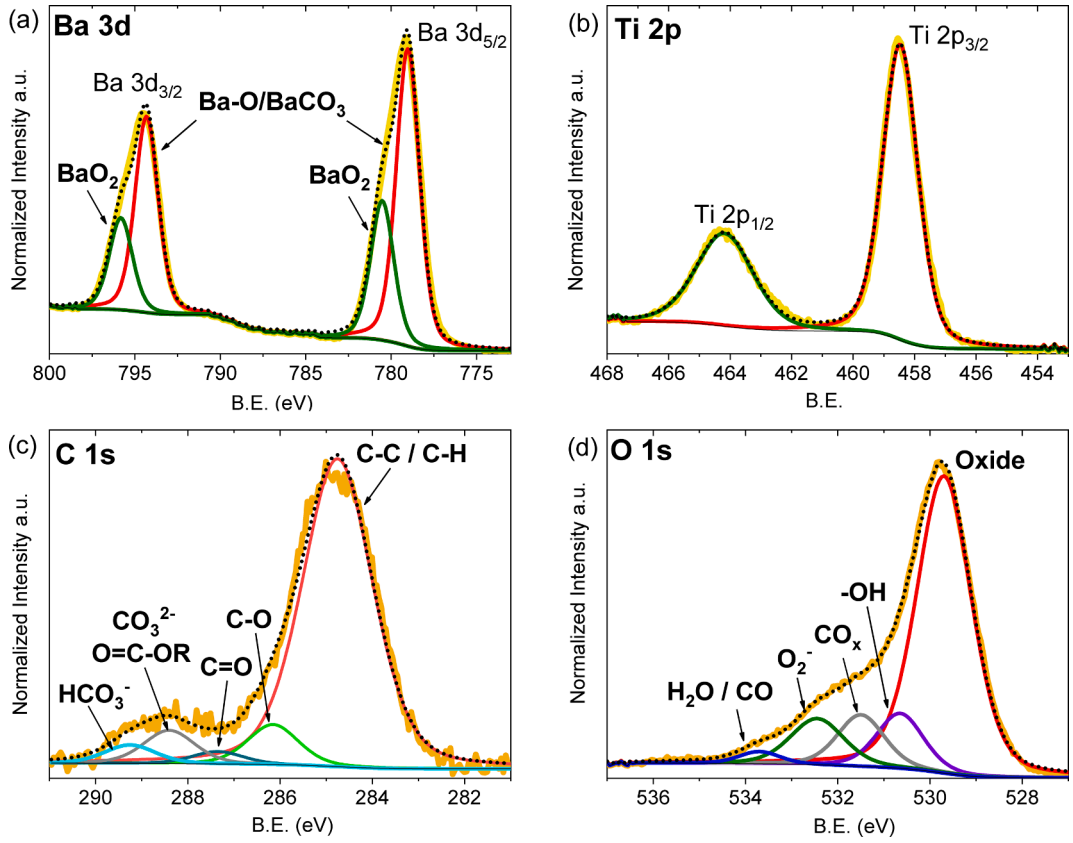

Fig. 3. Decomposition of XPS spectra at Ba 3d (a), Ti 2p (b), C 1s (c) and O 1s (d) regions of as-grown up-polarized $BaTiO_3$ thin film after being exposed to the air during 20 min, revealing contributions from undissociated water molecules, hydroxyl (OH) groups, peroxide species (Surface O_2^-) and different carbon-related species (CO_x) (see detailed explanation in the text).

coupled scan recorded around the (002) reflection in the 39^0 – 49^0 range shows three peaks belonging to tetragonal structure of $BaTiO_3$ and orthorhombic structure of $SrRuO_3$ thin films, as well as a peak that stems from $SrTiO_3$ substrate (Fig. 1a). Out-of-plane lattice parameters have values of c_{SRO} = 3.955 Å for $SrRuO_3$ and c_{BTO} = 4.149 Å for $BaTiO_3$ thin film, respectively. These values are in agreement with the values reported in literature for the fully strained $SrRuO_3/BaTiO_3$ bilayers grown on $SrTiO_3$ (100) substrates [31]. The results from reflectivity measurements (Fig. 1b) were analyzed by X'Pert Reflectivity Software (Malvern-Panalytical) and common Fourier method from which we obtained a thickness of 33 nm for the $SrRuO_3$ and 21 nm for the $BaTiO_3$ layer, respectively.

In order to investigate the strain state of epitaxial $SrRuO_3/BaTiO_3$ bilayers we have recorded X-Ray reciprocal space map (XRSM) around (-103) $SrTiO_3$ Bragg reflection. From this measurement is evident that $SrRuO_3$ and $BaTiO_3$ layers are coherent and fully strained to the single crystal $SrTiO_3$ substrate (Fig. 1c). The in-plane lattice parameter of both layers is 3.905 Å and it is equal to the in-plane lattice parameter of $SrTiO_3$ substrate. c/a ratio for $BaTiO_3$ thin film is 1.06, therefore showing c-orientation of the $BaTiO_3$ film. The topography of the as-grown thin film was imaged by AFM tapping mode (Fig. 2a). On the surface of the film some atomic step-terrace structures are visible, which is characteristic of layer-by-layer growth, but also some holes. Root-mean square surface roughness (R_{rms}) is about 0.4 nm.

The PFM phase image of as-grown and electrically written ferroelectric domains is presented in Fig. 2b. In order to check the as-grown polarization state, we electrically write two squares of opposite polarization by applying a DC voltage to the tip of V_{tip} = + 8 V (forcing the

polarization down) and V_{tip} = – 8 V (forcing the polarization to switch up) while scanning in contact over an area of 3.5 x 3.5 μm^2 and 1 x 1 μm^2 respectively. Since the phase contrasts of the inner square polarized with – 8 V and that of background are the same, we can conclude that the as-grown $BaTiO_3$ thin film is out-of-plane up-polarized, as expected for the $BaTiO_3$ films grown under compressive strain on this electrode [31].

Finally, we study the pristine-like surface composition of an as-grown sample (Sample A), transferred to XPS chamber within 20 min after growth in order to minimize time of exposure to ambient conditions. Fig. 3 shows the XPS spectra of an up-polarized $BaTiO_3$ thin film at the Ba 3d (a), Ti 2p (b), C 1s (c) and O 1s (d) regions. The Ti 2p spectrum has been deconvoluted into the characteristic spin–orbit split doublet. The Ti $2p_{3/2}$ peak has a main component at 458.8 eV due to Ti^{4+} valence state. The presence of possible surface oxygen vacancies can be determined by existence of shoulder in the low BE side of the Ti^{4+} $2p_{3/2}$ peak which would correspond to reduced Ti^{3+}. The absence of a Ti^{3+} peak is in line with the absence of oxygen vacancies close to the surface, within the limit of detection of our XPS equipment.

The complex structure of the O 1s spectrum shown in Fig. 3d was fitted using the model explained in detail in reference [12]. Briefly, the lowest binding energy (BE) peak at 529.7 eV belongs to the oxide peak, while the higher BE peaks can be related to different adsorbates species present on the surface. Peak at ΔBE = + 0.95 eV has been associated to different types of hydroxyl OH groups on the surface bound to the metal, such as Ti- or Ba-bonded terminal OH groups (Ti—**O**H, Ba—**O**H) and bridging hydroxyl groups (**Ox**-H). The peak at ΔBE = + 1.8 eV from the main oxide peak has been associated to different carbon-related species CO_x such as carbonates CO_3^{2-}, C=**O** bonds, ester (C—(C=**O**)—OR) or carboxylic acid (C—(C=**O**)—OH) compounds. Following peak at ΔBE = + 2.75 eV, here named as "surface O_2^- peak", corresponds to chemisorbed oxygen species such as Ti-peroxo and -superperoxo complexes. It is worth to mention here that this specie is structurally similar to the oxygen in metal peroxides such as Ba**O**$_2$. Finally, a peak at ΔBE = + 4 eV, clearly observed in AP-XPS measurements in water atmosphere [7,12], has been usually associated with physisorbed molecular water bounded to other water molecules. However, C-**O** bonds from ester or carboxylic acid compounds can also contribute to the same peak as molecular water. From a depth profile analysis done by comparing the spectra taken at 0 deg with the one taken at 60 deg, and in agreement with the previously reported model [12], the OH species seem to be the ones close to the surface, followed by the carbonate and peroxide species, and all of them laying below the molecular water layer.

Finally, the he C 1s region has been fitted with four well-resolved peaks as shown in Fig. 3c. The peak at lowest binding energy of 284.8 eV belongs to C atoms attached to another C or H atom (**C**—C(H)). Components at ΔBE = + 1.4 eV and ΔBE = + 2.6 eV from the adventitious carbon peak are associated with C atom attached by single (**C**—O) or double bond (**C**=O) to O atom. The peak at ΔBE = + 3.65 eV can be related with C atom in carbonate (**C**O_3^{2-}), ester (C—(**C**=O)—OR) or carboxylic acid (C—(**C**=O)—OH) compounds [32]. Finally, the peak at highest binding energy ΔBE = + 4.5 eV that is observed only in some cases has been related with the presence of bicarbonates (HCO_3^-).

Spectrum in the Ba 3d region exhibits the typical $3d_{3/2}$ and $3d_{5/2}$ doublet, which can be further resolved in two different contributions. The peak at the lowest BE of 779.0 eV (for the Ba $3d_{5/2}$) belongs to Ba atoms in the oxide lattice. A second peak is observed at a higher BE, i.e. ΔBE = + 1.5 eV shifted from the main peak. By comparing the spectra taken at 0 deg with the one taken at 60 deg, with higher surface sensitivity, we have extracted a depth profile and observed that this second specie is much more superficial than the main Ba peak. Hitherto, the assignment of this peak has been controversial and remains still under debate: it is generally attributed to Ba in surface compounds in which Ba has different oxygen coordination than in the bulk, such as barium carbonate $BaCO_3$ or barium hydroxide $Ba(OH)_2$. However, these findings are not justified, since the peak at ≈ + 1.5 eV from BaO is observed in many samples and in a lot of cases exists even when carbonate species

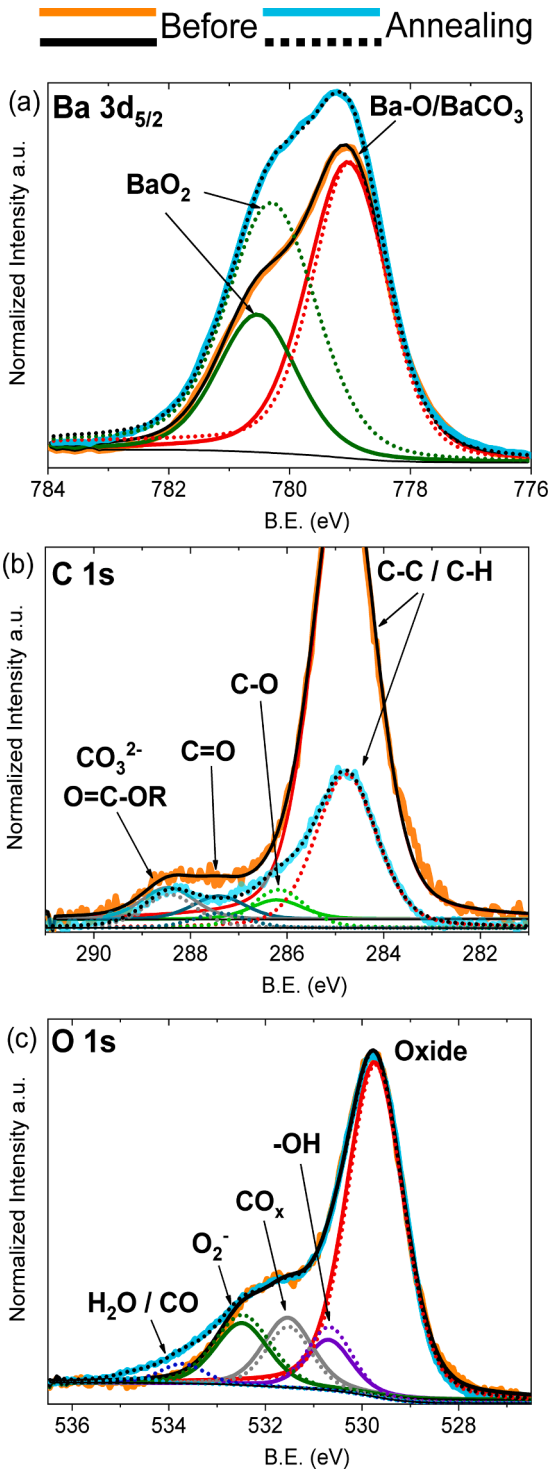

Fig. 4. Decomposition of XPS spectra at the Ba 3d (a), C 1s (b) and O 1s (c) regions, taken in vacuum conditions at RT and with an incident angle of 60° (increased surface sensitivity) of an up-polarized $BaTiO_3$ sample. The spectra are taken before (full orange lines) and after (blue dotted lines) annealing the sample at 250 °C in saturated O_2 atmosphere. . Ba $3d_{5/2}$ spectra show that annealing causes an increment of the component at + 1.5 eV from BaO peak, which is in direct relation with the increment of surface O_2^- peak at + 2.75 eV from main oxide peak in O 1s region and therefore can be related with the presence of BaO_2. (For interpretation of the references to colour in this figure legend, the reader is referred to the web version of this article.)

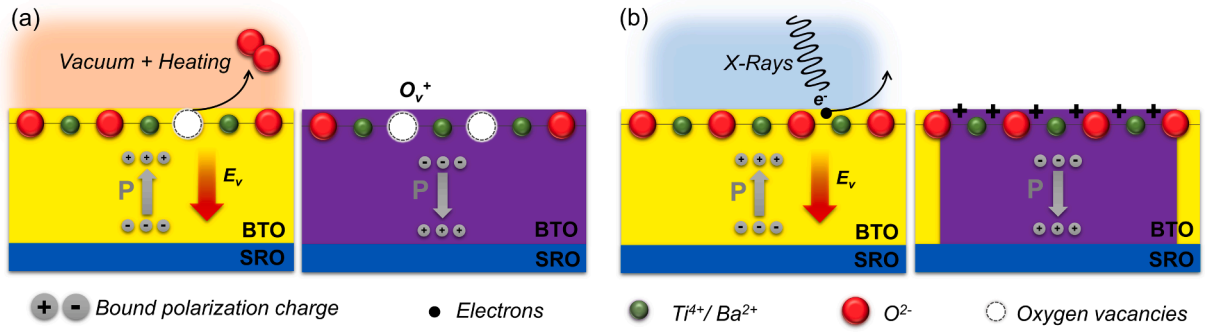

Fig. 5. Schematic representation of polarization switching from up to down state, caused by formation of positive electric field E_v associated with (a) creation of surface oxygen vacancies O_v^+ due to vacuum annealing or (b) creation of electron vacancies due to X-rays photoelectronic excitations, leading to positive surface charging.

cannot be detected by XPS (i.e. in C 1s or O 1s spectra) nor by IR measurements at the surface [16,26,28,33]. Moreover, the oxidation environment of Ba in $BaCO_3$ molecules should be similar to that of the bulk, so any contribution should be located close to or overlapping with the main oxide peak. Nonetheless, this peak has also been observed for $BaTiO_3$ single crystals cleaved in vacuum conditions, where no external molecules were available to interact with the surface [34]. Therefore, the component at higher BE cannot be univocally related to the presence of $BaCO_3$ species. On another hand, the presence of previously proposed $Ba(OH)_2$ [28] is improbable in the case of samples exposed to ambient, since CO_2 from the atmosphere would react instantaneously with Ba $(OH)_2$ forming $BaCO_3$ following the reaction: $Ba(OH)_2 + CO_2 \rightarrow BaCO_3 + H_2O$ [26]. Furthermore, in literature one can see that the high energy Ba $3d_{5/2}$ peak is always followed by the presence of another peak in the O1s spectrum at $\Delta BE = +2.8$ eV ($\pm$ 0.1 eV) from the main oxide peak, which in the corresponding literature is arbitrary associated to surface OH groups or carbonate species [20,28,30,35]. In our previous studies of oxide perovskite surfaces in water vapor atmosphere, we demonstrated that surface OH peak is placed rather closely to the oxide peak, giving that its intensity was uniformly increasing as water was dosed into the chamber [7]. Therefore, peak at $\Delta BE = +2.8$ eV from oxide cannot be related to OH groups or carbonate species.

In this work, we prove that the high energy component of Ba $3d_{5/2}$ peak corresponds to BaO_2. On one hand, the works [35,36] show that the BE of BaO_2 is expected to be shifted by $\Delta BE = 1.3$–1.7 eV from the BaO compound, in agreement with our observations. In addition, the presence of the high energy peak in Ba 3d spectrum in our case is also clearly associated with the presence of the peak at $\Delta BE = +2.8$ eV from oxide in the O1s spectrum, which we previously attributed to peroxide species [12] in agreement to what should be expected from BaO_2. Significant amount of BaO_2 on our $BaTiO_3$ surfaces might be related with the sample preparation method: after the thin film growth at 700 °C, the chamber is saturated with O_2 while the temperature is ramped down very slowly (3 °C/min). These conditions of high O_2 pressure and temperature can foster the production of BaO_2 by, for example, following the reaction $2BaO + O_2 \rightarrow 2BaO_2$, and therefore this peak might not be present on samples made by different procedures.

Finally, taking into account clear evidence of a CO_3^{2-} peak in the C 1s and O 1s regions, we cannot neglect the presence of $BaCO_3$. Still, as mentioned before, the position of this peak in the Ba 3d spectrum can probably overlap that of the $BaTiO_3$ position [37,38] from the bulk contribution making it undetectable within our energy resolution.

So all in all, some few minutes of exposure to environmental conditions is enough for ferroelectric surfaces to react with water and hydrocarbon molecules from the atmosphere and create a layer of adsorbates: after 20 min in ambient conditions, the surface of our as-grown up polarized $BaTiO_3$ thin film contains hydroxyl groups obtained after water splitting reactions, BaO_2 and Ti-based peroxo complexes probably obtained after further oxidation of hydroxyl groups on the surface, and contains some degree of contamination in the form of carbonates.

3.2. Effect of annealing in O_2 atmosphere on surface chemistry

After the XPS characterization showed in Fig. 3, the sample was removed from XPS chamber and placed in an annealing chamber. Sample was annealed at 250 °C in saturated O_2 atmosphere ($P = 10^4$ mTorr) and afterwards cooled down slowly with a rate of 3 °C/min. After annealing treatment, sample was transferred to XPS chamber without breaking the vacuum by using a suitcase. Fig. 4 shows the Ba $3d_{5/2}$ (a), C 1s (b) and O 1s (c) XPS spectra of the $BaTiO_3$ thin film measured before and after the annealing treatment. By comparing the obtained Ba $3d_{5/2}$ spectrum after annealing with initial spectrum of this sample, it can be seen that the concentration of BaO_2 has strongly increased. The spectra at the C 1s region shows that annealing treatment diminishes the concentration of advantageous carbon as well as **C**═O bonds, while the peak corresponding to the $(\mathbf{C}O_3^{2-})$/(C═(**C**═O)═R) almost doesn't suffer any change. This can be due to the simultaneous effect of $\mathbf{C}O_3^{2-}$ species decrement and (C—(**C**═O)═R) species increment. At the same time, C**O**$_x$ peak in O1s region is decreased following the same trends observed for **C**═O and $(\mathbf{C}O_3^{2-})$/(C═(**C**═O)═R) peaks in C 1s region. Simultaneous decrement of CO_3^{2-} species and increment of BaO_2 can be explained by decomposition of carbonates at high temperatures on BaO and CO_2 ($BaCO_3 \rightarrow BaO + CO_2$), whereby free BaO terminations can be further oxidized to BaO_2 and CO_2 pumped away from the XPS chamber. This oxidation also impacts as an increment of the surface O_2^- peak in the O 1s spectrum. The formation of BaO_2 species gives rise to the surface O_2^- peak evidencing the interconnected behavior of these two peaks (note that in this case, the rise of surface O_2^- peak is not coming due to dissociative water surface oxidation reactions). This experiment confirms that the peak at $\Delta BE = +1.5$ eV from the main peak in the Ba 3d region corresponds to the BaO_2 species and is entangled to the component at $\Delta BE = +2.8$ eV from the main peak in the O 1s. Therefore, it can additionally be used to specifically follow this oxidative reaction as a function of time and polarization.

3.3. Environmental assisted polarization switching

The polarization state of our as grown up-polarized samples is shown to be prone to reverse under specific environmental conditions and under X-Ray exposure: when exposed to temperatures up to 200 °C in vacuum or when irradiated with X-Rays in the frame of an XPS experiment in vacuum conditions, we observe a switching of the polarization state in the whole area of the sample, as probed by PFM (images not shown here).

This switching can be attributed generically to the creation of a positive surface potential as shown in Fig. 5a,b by a) the formation of oxygen vacancies at the surface during vacuum annealing process or b)

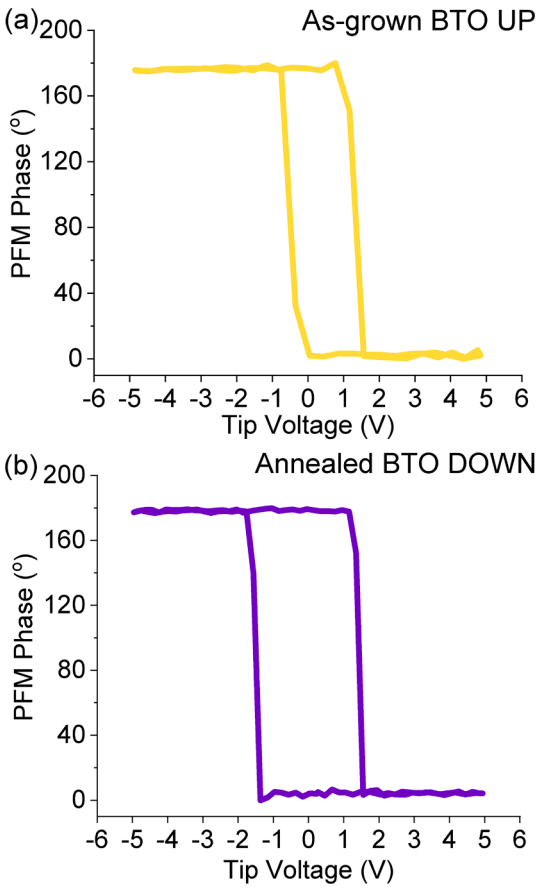

Fig. 6. SS-PFM hysteresis loops of (a) as grown up-polarized $BaTiO_3$ thin film, showing coercive voltage of $V_{c,\ up} = 1.2$ V with a slightly positive bias of $V_{bias,\ up} = 0.4$ V and (b) switched down-polarized $BaTiO_3$ thin film obtained after vacuum annealing, with increased coercive voltage of $V_{c,\ down} = 1.4$ V and almost no bias. As a consequence of polarization switching, the internal bias disappears leading ultimately to a more robust polarization as observed by the increase of coercive voltage and absence of bias.

the creation of electron vacancies during the XPS measurements. In both cases, this favors ferroelectric switching.

Polarization switching might be an inherent part of XPS experiments when the size of X-Ray beam spot arriving to the sample is comparable to sample size, in a way that X-ray photons that are removing photoelectrons from the sample are leaving behind positively charged holes. These holes can be easily filled by negative charge carriers present in the highly conductive metallic samples, but not in the case of insulating samples such as ours. Negative charge needed for holes' compensation might come from the bottom $SrRuO_3$ electrode, however these electrons might recombine with positive charge carriers on their way to the top layers of the sample, making this process highly ineffective. In that case uncompensated positive holes on the surface would create electric field E_v, opposing the as-grown polarization of the sample, which could switch it down. These processes are schematically depicted in Fig. 5a,b. In a similar way, annealing in vacuum conditions up to 200 °C can create a positive surface voltage either by inducing new oxygen vacancies or by removing essential screening charges that can lead to ferroelectric polarization switching.

Fig. 6a,b show the PFM hysteresis cycles of as-grown up polarized and a switched sample after vacuum annealing. The as-grown sample shows a coercive voltage of $V_{c,\ up} = 1.2$ V with a slightly positive bias of $V_{bias,\ up} = 0.4$ V. This initial positive bias denotes the presence of a built-in down electric field on the as-grown sample that probably nucleates the as-grown up polarization state. This field can be related with the accumulation of positive charge at the interface between the film and

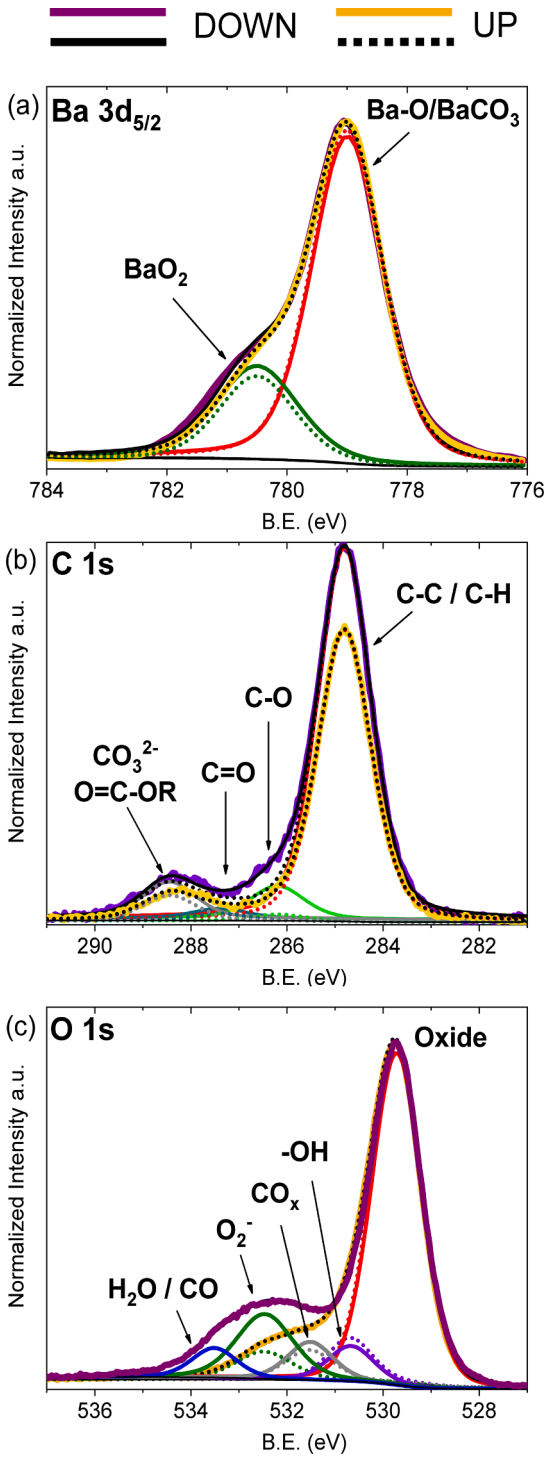

Fig. 7. Decomposition of XPS spectra at the Ba 3d (a), C 1s (b) and O 1s (c) regions, taken in vacuum conditions at RT for down- (purple, full lines) and up- (yellow, dotted lines) polarized $BaTiO_3$ samples after being exposed to ambient conditions during a period of several months. Compared to the spectra taken on as grown up-polarized $BaTiO_3$ shown in Fig. 3, long exposure to ambient conditions leads to increment of adventitious carbon, carbonates and also surface oxygen species dominated by Ti-peroxo complexes. Interestingly, this increment is clearly more pronounced for down-polarized sample, which is represented in Table 1. (For interpretation of the references to colour in this figure legend, the reader is referred to the web version of this article.)

Table 1
Relative increase of the ratios of the species in O 1s, Ba $3d_{5/2}$ and C 1s regions of $BaTiO_3$ thin films due to prolonged time exposure and as a function of polarization, when compared with an as-grown sample. The ratio of the oxygen species is taken by dividing the areas of the peaks with the area of the main oxide peak, corresponding to bulk BaO contribution; the ratio for Ba species is taken with respect to the main Ba peak, arising from the same contribution; and the ratios for carbon species are normalized again with respect to the main oxide peak area, taken as constant for all the samples. The first line shows the relative increase of species for an up polarized sample due to exposure to ambient conditions for three months, and the second line shows the relative increase in the species for a down polarized sample due to ambient exposure for four months, as compared to an as-grown sample.

Sample		O 1s			Ba $3d_{5/2}$	C 1s			
P state	Exposure to ambient	OH	COx	O_2^-	BaO_2	C-C	C-O	C=O	CO_3^{2-}
UP	3 Months	2.16%	2.65%	6.64 %	7.65 %	14.13 %	-0.80%	0.36%	1.05%
DOWN	4 Months	0.26 %	4.48%	20.14 %	13.68 %	20.40 %	1.20 %	0.55 %	1.89 %

the bottom electrode that might be in the form of oxygen vacancies. Instead, the switched sample shows an increase of stability as observed by a $V_{c,\ down} = 1.4$ V with almost no bias. Hysteresis loops obtained on switched samples after X-Ray exposure (not shown here) are showing the same trend of slight increase of coercive voltage and bias vanishing. Changes of ferroelectric hysteresis cycles can be explained as a consequence of polarization switching, after which interfacial oxygen vacancies can move from the bottom interface to the surface where they get cancelled by reacting with available oxide species, leading ultimately to a more robust polarization material as observed by the coercive voltage increase and the absence of bias in PFM hysteresis cycles.

3.4. *Effect of prolonged atmosphere exposure as a function of polarization state on $BaTiO_3$ thin films*

Fig. 7 shows the effect of atmospheric exposure on $BaTiO_3$ thin films surfaces as a function of their polarization state. Yellow lines show the XPS spectra at the Ba $3d_{5/2}$ (a), C 1s (b) and O 1s (c) regions of an as-grown up polarized sample after three months of exposure to ambient conditions (sample B). Purple lines show the XPS spectra of sample A, taken about four months after the spectra shown in Fig. 3. After the first XPS measurement we could see that polarization of sample A was switched, so that the sample has remained in a down polarized state for all this time. If we compare pristine $BaTiO_3$ film (Fig. 3) with long-term ambient exposed $BaTiO_3$, apparent changes in the Ba $3d_{5/2}$, C 1s and O 1s regions can be appreciated for both polarization states. Table 1 shows the change in the ratios of peaks as a function of time for the different polarization states. For both samples, the amount of BaO_2 on the surface is increasing during the time, but the down polarized surface seems to be more reactive. Increment of $BaCO_3$ is also observable in the C 1s and O 1s region by following CO_3^{2-} and CO_x peaks, respectively, with higher peaks for the down polarized surface. Surface O_2^- peak in O 1s spectrum shows the behavior of surface peroxide species. Here we see that during the ambient exposure surface O_2^- peak is increasing for both surfaces, being the negative polarized surface again the one showing higher reactivity. This peak should include the contribution from both, BaO_2 and Ti-peroxo complexes. In the case of complex water-assisted surface reactions, analysis of Ba $3d_{5/2}$ region can thus provide additional information regarding surface oxygen state, which is not always achievable only from O 1s region. Since we can isolate the contribution from the increase of the BaO_2 peak in the Ba $3d_{5/2}$ spectrum, this allows us to directly monitor the Ba driven electrochemical reactions as a function of polarization.

Surface oxidation on the different metal active sites follows different reactions. Ti sites in TiO_2 terminated surfaces are known to be very reactive to water. They will mainly catalyze water splitting leading to strong surface hydroxylation. Furthermore, negative polarized surfaces lead to oxidative water adsorption; in this process terminal-OH groups are further oxidized to Ti –peroxo and –superperoxo complexes, which also results in increment of surface O_2^- peak. Instead, Ba sites in BaO terminated surfaces are not able to build stable metal-peroxo complexes like Ti atoms. In this case reaction with O_2 from atmosphere is more probable to take place, giving rise to BaO_2 and surface O_2^- peaks but with much smaller reactivity rates. This reaction normally proceeds at increased temperatures as demonstrated earlier, however it has also been reported when electric potential of several hundreds of millivolts is applied [39].

In comparison to other oxide materials, ferroelectrics have an additional degree of freedom, i.e. polarization which can take different orientations and therefore affect sign of the surface screening charge (i.e. electric field). In that sense, screening charge act as an active layer, which is able to accommodate or supply negative charge and therefore take part in electrochemical reactions happening on the surface: down-polarized surface with positive surface electric field act as anode by being able to accept electrons produced in surface oxidation processes. In the case of $BaTiO_3$, positive anodic potential on ferroelectric surface might catalyze oxidation reaction in which oxygen atoms change valence state from −2 in BaO to −1 in BaO_2. Besides, down-polarized surfaces will also be able to accommodate the generated electrons formed by the oxidation of OH groups (i.e. loss of H atoms and electrons) during the formation of Ti-peroxo and –superperoxo species.

Our results show that long exposure of $BaTiO_3$ ferroelectric surfaces to ambient conditions during prolonged periods of time leads mainly to an increment of Ti-peroxo species especially pronounced on the down-polarized surfaces (as observed by a drastic increment of surface O_2^- peak), together with some increase of BaO_2. Altogether, this turns down polarized surfaces into more hydrophilic ones, probably due to the hydrogen bonds formation between water molecules and surface oxygen species. This agrees with water adsorption study on PZT thin films [8], which shows that indeed down-polarized surfaces have more hydrophilic character as compared to up-polarized ones. It is to mention that probably, as also observed for PZT, once this adsorbates layer is formed upon time as a function of the polarization state, it cannot be reversibly switched and remains there as an imprint of the sample's ferroelectric state history [8].

4. Conclusions

In this work, we have demonstrated that $BaTiO_3$ thin film surfaces are easily oxidized in different possible ways after exposure to ambient conditions, and that oxidative reactions strongly depend on the active surface sites involved. It is especially remarkable the formation of BaO_2 species happening in almost every $BaTiO_3$ surface which was neglected up to now and has been demonstrated to be fostered by annealing processes in O_2 atmosphere. The identification of this new surface component on $BaTiO_3$ surfaces is very relevant for the study of screening

mechanisms of this ferroelectric material and in views of its application for catalysis processes.

Long exposure to ambient conditions of $BaTiO_3$ surfaces leads to: i) increment of BaO_2 as observed from Ba $3d_{5/2}$ region and ii) formation of Ti -peroxo and -superperoxo compounds which are dominating the behavior of surface O_2^- peak in O 1s region. But still, down polarized surfaces foster these oxidative water adsorption reactions by being able to accept electrons due to positive screening charge in the surface region as compared with up polarized surfaces. In this way, down polarized surfaces act as catalyzers of oxidative water adsorption reactions and become thereby also more hydrophilic.

Finally, we have observed that our as-grown $BaTiO_3$ thin films are polarized up due to a negative built-in electric field, observed as a positive bias in the PFM hysteresis cycle, probably due to the accumulation of positive charge at the bottom electrode in the form of oxygen vacancies. Cancelation of this built-in field by the displacement of oxygen vacancies to the surface due to the generation of positive voltages at the surface under X-Ray exposure or under annealing in vacuum turns into the spontaneous switching of ferroelectric polarization to a down state.

CRediT authorship contribution statement

Irena Spasojevic: Investigation, Resources, Methodology, Conceptualization, Writing - original draft, Visualization. **Guillaume Sauthier:** Resources, Investigation. **José Manuel Caicedo:** Resources, Investigation. **Albert Verdaguer:** Conceptualization, Validation. **Neus Domingo:** Supervision, Conceptualization, Validation, Formal analysis, Writing - review & editing, Funding acquisition.

Declaration of Competing Interest

The authors declare that they have no known competing financial interests or personal relationships that could have appeared to influence the work reported in this paper.

Acknowledgements

Financial support was obtained under projects from the Spanish Ministerio de Ciencia e Innovación (MICINN) under projects FIS2015-73932-JIN, PID2019-109931GB-I00 and PID2019-110907GB-I00. In addition, this work was partially funded by 2017-SGR-579 from the Generalitat de Catalunya. The ICN2 is funded by the CERCA programme/Generalitat de Catalunya. The ICN2 is supported by the Severo Ochoa Centres of Excellence Programme, funded by the Spanish Research Agency (AEI, grant no. SEV-2017-0706) and ICMAB is supported by the Severo Ochoa Centres of Excellence Programme, funded by the Spanish Research Agency (AEI, grant no. CEX2019-000917-S). I. S. acknowledges support of the Secretaria d'Universitats i Recerca - Departament d'Empresa i Coneixement - Generalitat de Catalunya and the European Social Fund (ESF) (FI grant reference 2020 FI_B2 00157).

References

[1] L. Chen, L. Qian, Role of interfacial water in adhesion, friction, and wear—A critical review, Friction 9 (2021) 1–28, https://doi.org/10.1007/s40544-020-0425-4.
[2] K. Iwahori, S. Watanabe, M. Kawai, K. Kobayashi, H. Yamada, K. Matsushige, Effect of water adsorption on microscopic friction force on $SrTiO_3$(001), J. Appl. Phys. 93 (2003) 3223–3227, https://doi.org/10.1063/1.1540223.
[3] J.J. Segura, N. Domingo, J. Fraxedas, A. Verdaguer, Surface screening of written ferroelectric domains in ambient conditions, J. Appl. Phys. 113 (2013), 187213, https://doi.org/10.1063/1.4801983.
[4] H. Lee, T.H. Kim, J.J. Patzner, H. Lu, J.W. Lee, H. Zhou, W. Chang, M. K. Mahanthappa, E.Y. Tsymbal, A. Gruverman, C.B. Eom, Imprint Control of $BaTiO_3$ Thin Films via Chemically Induced Surface Polarization Pinning, Nano Lett. 16 (2016) 2400–2406, https://doi.org/10.1021/acs.nanolett.5b05188.
[5] C. Blaser, P. Paruch, Subcritical switching dynamics and humidity effects in nanoscale studies of domain growth in ferroelectric thin films, New J. Phys. 17 (2015) 013002, https://doi.org/10.1088/1367-2630/17/1/013002.
[6] A.V. Ievlev, A.N. Morozovska, V.Y. Shur, S.V. Kalinin, A.V. Ievlev, A. N. Morozovska, V.Y. Shur, S.V. Kalinin, Humidity effects on tip-induced polarization switching in lithium niobate, Appl. Phys. Lett. 104 (2014), 092908, https://doi.org/10.1063/1.4867979.
[7] K. Cordero-Edwards, L. Rodríguez, A. Calò, M.J. Esplandiu, V. Pérez-Dieste, C. Escudero, N. Domingo, A. Verdaguer, Water Affinity and Surface Charging at the z-Cut and y-Cut $LiNbO_3$ Surfaces: An Ambient Pressure X-ray Photoelectron Spectroscopy Study, J. Phys. Chem. C. 120 (2016) 24048–24055, https://doi.org/10.1021/acs.jpcc.6b05465.
[8] N. Domingo, I. Gaponenko, K. Cordero-Edwards, N. Stucki, V. Pérez-Dieste, C. Escudero, E. Pach, A. Verdaguer, P. Paruch, Surface charged species and electrochemistry of ferroelectric thin films, Nanoscale 11 (2019) 17920–17930, https://doi.org/10.1039/c9nr05526f.
[9] S. Sanna, R. Hölscher, W.G. Schmidt, Polarization-dependent water adsorption on the $LiNbO_3$(0001) surface, Phys. Rev. B - Condens. Matter Mater. Phys. 86 (2012), 205407, https://doi.org/10.1103/PhysRevB.86.205407.
[10] M.H. Zhao, D.A. Bonnell, J.M. Vohs, Effect of ferroelectric polarization on the adsorption and reaction of ethanol on $BaTiO_3$, Surf. Sci. 602 (2008) 2849–2855, https://doi.org/10.1016/j.susc.2008.07.011.
[11] D. Li, M.H. Zhao, J. Garra, A.M. Kolpak, A.M. Rappe, D.A. Bonnell, J.M. Vohs, Direct in situ determination of the polarization dependence of physisorption on ferroelectric surfaces, Nat. Mater. 7 (2008) 473–477, https://doi.org/10.1038/nmat2198.
[12] N. Domingo, E. Pach, K. Cordero-Edwards, V. Pérez-Dieste, C. Escudero, A. Verdaguer, Water adsorption, dissociation and oxidation on $SrTiO_3$ and ferroelectric surfaces revealed by ambient pressure X-ray photoelectron spectroscopy, Phys. Chem. Chem. Phys. 21 (2019) 4920–4930, https://doi.org/10.1039/c8cp07632d.
[13] G. Geneste, B. Dkhil, Adsorption and dissociation of H_2O on in-plane-polarized $BaTiO_3$ (001) surfaces and their relation to ferroelectricity, Phys. Rev. B - Condens. Matter Mater. Phys. 79 (2009), 235420, https://doi.org/10.1103/PhysRevB.79.235420.
[14] X. Li, B. Wang, T.Y. Zhang, Y. Su, Water adsorption and dissociation on $BaTiO_3$ single-crystal surfaces, J. Phys. Chem. C. 118 (2014) 15910–15918, https://doi.org/10.1021/jp5051386.
[15] I. Efe, N.A. Spaldin, C. Gattinoni, On the happiness of ferroelectric surfaces and its role in water dissociation: The example of bismuth ferrite, J. Chem. Phys. 154 (2021), 024702, https://doi.org/10.1063/5.0033897.
[16] J.L. Wang, F. Gaillard, A. Pancotti, B. Gautier, G. Niu, B. Vilquin, V. Pillard, G.L.M. P. Rodrigues, N. Barrett, Chemistry and atomic distortion at the surface of an epitaxial $BaTiO_3$ thin film after dissociative adsorption of water, J. Phys. Chem. C. 116 (2012) 21802–21809, https://doi.org/10.1021/jp305826e.
[17] L.E. Ştoflea, N.G. Apostol, L. Trupină, C.M. Teodorescu, Selective adsorption of contaminants on Pb(Zr, Ti)O_3 surfaces shown by X-ray photoelectron spectroscopy, J. Mater. Chem. A. 2 (2014) 14386–14392, https://doi.org/10.1039/c4ta02660h.
[18] Y. Cui, J. Briscoe, S. Dunn, Effect of ferroelectricity on solar-light-driven photocatalytic activity of $BaTiO_3$ - Influence on the carrier separation and stern layer formation, Chem. Mater. 25 (2013) 4215–4223, https://doi.org/10.1021/cm402092f.
[19] M. Wang, B. Wang, F. Huang, Z. Lin, Enabling PIEZOpotential in PIEZOelectric Semiconductors for Enhanced Catalytic Activities, Angew. Chemie - Int. Ed. 58 (2019) 7526–7536, https://doi.org/10.1002/anie.201811709.
[20] J.L. Wang, B. Vilquin, N. Barrett, Screening of ferroelectric domains on $BaTiO_3$(001) surface by ultraviolet photo-induced charge and dissociative water adsorption, Appl. Phys. Lett. 101 (2012), 092902, https://doi.org/10.1063/1.4748330.
[21] Y. Zhang, M. Xie, V. Adamaki, H. Khanbareh, C.R. Bowen, Control of electrochemical processes using energy harvesting materials and devices, Chem. Soc. Rev. 46 (2017) 7757–7786, https://doi.org/10.1039/c7cs00387k.
[22] A. Kakekhani, S. Ismail-Beigi, Polarization-driven catalysis: Via ferroelectric oxide surfaces, Phys. Chem. Chem. Phys. 18 (2016) 19676–19695, https://doi.org/10.1039/c6cp03170f.
[23] A. Kakekhani, S. Ismail-Beigi, E.I. Altman, Ferroelectrics: A pathway to switchable surface chemistry and catalysis, Surf. Sci. 650 (2016) 302–316, https://doi.org/10.1016/j.susc.2015.10.055.
[24] N.Z. Koocher, J.M.P. Martirez, A.M. Rappe, Theoretical model of oxidative adsorption of water on a highly reduced reconstructed oxide surface, J. Phys. Chem. Lett. 5 (2014) 3408–3414, https://doi.org/10.1021/jz501635f.
[25] J.M.P. Martirez, S. Kim, E.H. Morales, B.T. Diroll, M. Cargnello, T.R. Gordon, C. B. Murray, D.A. Bonnell, A.M. Rappe, Synergistic oxygen evolving activity of a TiO_2-rich reconstructed $SrTiO_3$(001) surface, J. Am. Chem. Soc. 137 (2015) 2939–2947, https://doi.org/10.1021/ja511332y.
[26] S. Kumar, V.S. Raju, T.R.N. Kutty, Investigations on the chemical states of sintered barium titanate by X-ray photoelectron spectroscopy, Appl. Surf. Sci. 206 (2003) 250–261, https://doi.org/10.1016/S0169-4332(02)01223-0.
[27] A. Pancotti, J. Wang, P. Chen, L. Tortech, C.M. Teodorescu, E. Frantzeskakis, N. Barrett, X-ray photoelectron diffraction study of relaxation and rumpling of ferroelectric domains in $BaTiO_3$(001), Phys. Rev. B - Condens. Matter Mater. Phys. 87 (2013), 184116, https://doi.org/10.1103/PhysRevB.87.184116.
[28] J.L. Wang, J. Leroy, G. Niu, G. Saint-Girons, B. Gautier, B. Vilquin, N. Barrett, Chemistry and structure of $BaTiO_3$ ultra-thin films grown by different O_2 plasma power, Chem. Phys. Lett. 592 (2014) 206–210, https://doi.org/10.1016/j.cplett.2013.12.030.

[29] C. Miot, E. Husson, C. Proust, R. Erre, J.P. Coutures, Residual Carbon Evolution in $BaTiO_3$ Ceramics Studied by XPS after Ion Etching, J. Eur. Ceram. Soc. 18 (1998) 339–343, https://doi.org/10.1016/S0955-2219(97)00119-2.
[30] C.C. Li, S.J. Chang, J.T. Lee, W.S. Liao, Efficient hydroxylation of $BaTiO_3$ nanoparticles by using hydrogen peroxide, Colloids Surf. A Physicochem. Eng. Asp. 361 (2010) 143–149, https://doi.org/10.1016/j.colsurfa.2010.03.027.
[31] P. Zubko, H. Lu, C.W. Bark, X. Martí, J. Santiso, C.B. Eom, G. Catalan, A. Gruverman, On the persistence of polar domains in ultrathin ferroelectric capacitors, J. Phys. Condens. Matter. 29 (2017), 284001, https://doi.org/10.1088/1361-648X/aa73c3.
[32] J. Landoulsi, M.J. Genet, S. Fleith, Y. Touré, I. Liascukiene, C. Méthivier, P. G. Rouxhet, Organic adlayer on inorganic materials: XPS analysis selectivity to cope with adventitious contamination, Appl. Surf. Sci. 383 (2016) 71–83, https://doi.org/10.1016/j.apsusc.2016.04.147.
[33] V. Craciun, R.K. Singh, Characteristics of the surface layer of barium strontium titanate thin films deposited by laser ablation, Appl. Phys. Lett. 76 (2000) 1932–1934, https://doi.org/10.1063/1.126216.
[34] L.T. Hudson, R.L. Kurtz, S.W. Robey, D. Temple, R.L. Stockbauer, Surface core-level shifts of barium observed in photoemission of vacuum-fractured $BaTiO_3$(100), Phys. Rev. B. 47 (1993) 10832–10838, https://doi.org/10.1103/PhysRevB.47.10832.
[35] S. Chakrabarti, S. Ginnaram, S. Jana, Z.Y. Wu, K. Singh, A. Roy, P. Kumar, S. Maikap, J.T. Qiu, H.M. Cheng, L.N. Tsai, Y.L. Chang, R. Mahapatra, J.R. Yang, Negative voltage modulated multi-level resistive switching by using a Cr/$BaTiO_x$/TiN structure and quantum conductance through evidence of H_2O_2 sensing mechanism, Sci. Rep. 7 (2017), 4735, https://doi.org/10.1038/s41598-017-05059-9.
[36] T.C. Droubay, L. Kong, S.A. Chambers, W.P. Hess, Work function reduction by BaO: Growth of crystalline barium oxide on Ag(001) and Ag(111) surfaces, Surf. Sci. 632 (2015) 201–206, https://doi.org/10.1016/j.susc.2014.07.010.
[37] R.P. Vasquez, X-ray photoelectron spectroscopy study of Sr and Ba compounds, J. Electron Spectros. Relat. Phenomena. 56 (1991) 217–240, https://doi.org/10.1016/0368-2048(91)85005-E.
[38] P.J. Schmitz, Characterization of the Surface of $BaCO_3$ Powder, Surf. Sci. Spectra. 190 (2002) 190–194, https://doi.org/10.1116/11.20011102.
[39] D. Kim, R. Bliem, F. Hess, J.J. Gallet, B. Yildiz, Electrochemical Polarization Dependence of the Elastic and Electrostatic Driving Forces to Aliovalent Dopant Segregation on $LaMnO_3$, J. Am. Chem. Soc. 142 (2020) 3548–3563, https://doi.org/10.1021/jacs.9b13040.